O-Space Turbo Spin Echo Imaging

Haifeng Wang[1], Leo Tam[1], Emre Kopanoglu[1], Dana Peters[1], R. Todd Constable[1], and Gigi Galiana[1]
[1]*Department of Diagnostic Radiology, Yale University, New Haven, CT, United States*

TARGET AUDIENCE: researchers interested in accelerated imaging and imaging with nonlinear gradients

PURPOSE: Turbo Spin Echo (TSE) sequences provide much faster scan time than standard spin echo sequences [1-2]. But artifacts can appear, since each sampled line is differently weighted by T2 effects. A more recently developed approach to faster imaging has been spatial encoding with nonlinear magnetic fields, such as PatLoc imaging [3], O-Space imaging [4], Null Space Imaging [5], or 4D-RIO [6]. Compared to methods using conventional linear gradient systems, these methods may require fewer echoes in the presence of multiple receiver coils. But most efforts to date have focused on gradient echo imaging. In this work, we present a hybrid of TSE and O-Space, developing an O-Space TSE sequence which is much faster than single echo O-Space imaging or conventional TSE. Various techniques are applied to overcome the problems of artifacts and ambiguous T2 weighting. Simulations and experiment illustrate that the proposed method can inherit the advantages of both TSE and O-Space.

METHODS: Some strategies are presented to accelerate imaging time and minimize image artifacts. Firstly, to reduce scan time of spin echo acquisitions, the most basic O-Space turbo spin echo (TSE) sequence is proposed in Fig. 1. In general, T2 decay imposes a magnitude weighting (approximately $e^{-TE/T2}$) on each acquired line in k-space per time of repetition (TR) dependent on TE [7]. In conventional TSE, T2-weighting is easily determined by the TE at which the $k_y = 0$ phase encode line is acquired. O-space imaging is a projection imaging sequence in which the center of k-space is acquired for each echo and the local k-space coverage typically differs for different parts of the image with each acquisition. Later, we will introduce a filtering strategy to control the echo time at which the low frequency information is allowed to contribute to the image contrast. With standard ordering (Fig.2 (a)), this weighting can create severe artifacts in O-Space images, but we minimize this effect by reordering the data acquisitions in each TR as shown in Fig.2 (b). Finally we apply a filtered Kaczmarz algorithm to reconstruct images [4, 8]. Assuming that β_i is the coefficient for the i-th encoding function, β_i is calculated as $\beta_i = D_i - A_i \cdot I_{i-1}$. Here A_i is the i-th encoding function; D_i is the measured data; I_{i-1} is the previous image estimate. Then the image is updated via $I_i = I_{i-1} + \lambda\beta_i A_i$, which ultimately minimizes $\|\mathbf{A}\cdot\mathbf{I} - \mathbf{D}\|_2$. Cycling through the entire dataset multiple times can further refine the estimate. Typically λ is a scalar relaxation parameter that controls convergence. However, the proposed reconstruction approach uses a filtered basis to reconstruct the image by making λ a function of x, y, and also $\boldsymbol{k} = (k_x, k_y, k_{z2})$, which corresponds to time. With this filter we can control the echo time at which low frequency information contributes to the final image, suppressing low spatial frequency information unless it is acquired near the desired time of echo (TE). For the time-varying filter, we define $\lambda(x, y, Echo) = \lambda_0\{1 - e^{-(|\mathbf{r}-\mathbf{CP}(Echo)|^2/\sigma(t)^2)}\}$, where $\mathbf{r}$ is the coordinates (x, y) of arbitrary data-point; $\mathbf{CP}(Echo)$ gives the coordinates of the gradient center placement for that echo; λ_0 expresses a scalar value; the function $\sigma(t)$ controls the width of the filter (except for data acquired from the target echo, in which case λ reverts to its scalar value) $\sigma(t) = \sigma_0\sqrt{\left(k_{x,max}^2 + k_{y,max}^2 + \left(\frac{FOV}{2}\right)k_{z2,max}^2\right)/\left(k_x^2 + k_y^2 + \left(\frac{FOV}{2}\right)k_{z2}^2\right)}$, especially when $k_x = k_y = k_{z2} = 0$, $\sigma(t) = \sigma_0$.

RESULTS: A simulation of a human brain imaging experiment is shown in Fig. 3. Here, all methods have an equal number of echoes (2 shots each with 16 echoes each of duration 7%×T2 and acquisition with 8 coils). Panel (a) is basic O-Space TSE; (b) is proposed O-Space TSE; (c) is Cartesian TSE. Two phantom datasets were obtained experimentally using a 3.0T Trio MRI scanner (Siemens Healthcare, Erlangen, Germany) with an 8-channel head coil and an O-Space gradient system. The sequence parameters are TE/TR: 12/200ms; BW: 390Hz/pixel; FOV: (25cm)^2; ETL: 4. We reconstructed both standard and proposed O-Space FSE images for 4 echoes collected over 128 shots, which is 4 times faster than the reference spin echo method. Fig. 4 shows, (a) standard O-Space TSE; (b) proposed O-Space TSE; (c) a reference. Therefore, the simulation and experimental results suggest that the proposed method decreases the aliasing artifacts caused by multi-echo acquisitions and improve SNR and image contrast, although the results show blurring caused by extremely fast T2 decay along the echo train seen in these preliminary results.

DISCUSSION AND CONCLUSION: The results from the both simulation and experiments illustrate that the proposed scheme presented here decreases the artifacts from multi-echo acquisition sequences with a faster imaging speed. Although a multi-echo acquisition of O-Space requires several modifications, the proposed sequence has the advantage of requiring fewer TRs and an overall shorter scan time than the standard O-Space spin echo sequences. In the preliminary results, pronounced T2 blurring remains due to a very short T2 in the phantom, which exacerbates the effects of the echo train. However, improvements from our modifications are still evident.

REFERENCES: **1**. Hennig et al., MRM 3(6): 823-833, 1986; **2**. Rasche et al., MRM 32(5): 629-638, 1994; **3**. Hennig et al., MAGMA 21(1-2): 5-14, 2008; **4**. Stockmann et al., MRM 64(2): 447-456, 2010; **5**. Tam et al., MRM 69(4): 1166-1175, 2012; **6**. Gallichan et al., MAGMA 25(6): 419-431, 2012; **7**. Constable et al., MRM 10(4): 497-511, 1992; **8**. Galiana et al., CMR Part A 40A(5): 253-267, 2012.

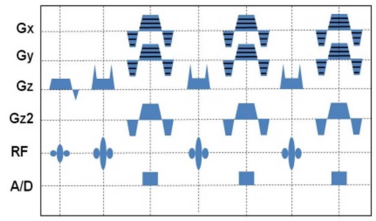

Fig.1 Timing diagram of proposed pulse sequence

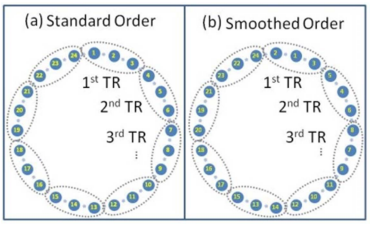

Fig.2 Rearranging View Order

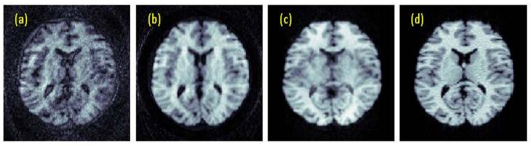

Fig.3 Simulation comparison of the standard (a), proposed (b), Cartesian (c), and reference (d) methods

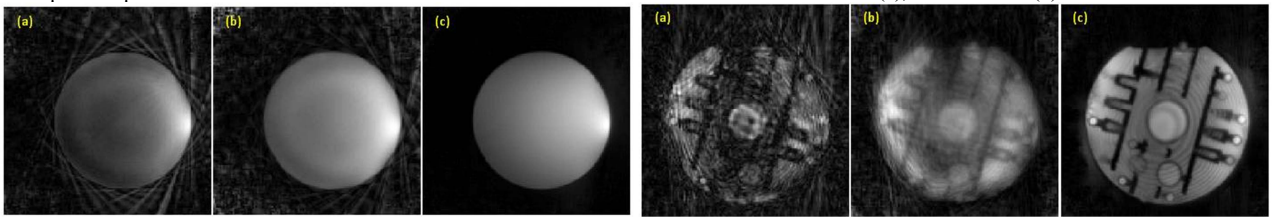

Fig.4 Two experimental comparisons of the standard (a), proposed (b) and reference (c)